



## NRC Publications Archive Archives des publications du CNRC

### **Optical coherence tomography used for jade industry**

Chang, Shoude; Mao, Youxin; Chang, Guangming; Flueraru, Costel

This publication could be one of several versions: author's original, accepted manuscript or the publisher's version. / La version de cette publication peut être l'une des suivantes : la version prépublication de l'auteur, la version acceptée du manuscrit ou la version de l'éditeur.

For the publisher's version, please access the DOI link below. / Pour consulter la version de l'éditeur, utilisez le lien DOI ci-dessous.

#### **Publisher's version / Version de l'éditeur:**

<https://doi.org/10.1117/12.868577>

*Proceeding of SPIE, 7855, 785514, pp. 785514-1-785514-9, 2010-10-18*

#### **NRC Publications Record / Notice d'Archives des publications de CNRC:**

<https://nrc-publications.canada.ca/eng/view/object/?id=8d16beec-9544-4c6c-92f9-e811bddd3b1>

<https://publications-cnrc.canada.ca/fra/voir/objet/?id=8d16beec-9544-4c6c-92f9-e811bddd3b1>

Access and use of this website and the material on it are subject to the Terms and Conditions set forth at

<https://nrc-publications.canada.ca/eng/copyright>

READ THESE TERMS AND CONDITIONS CAREFULLY BEFORE USING THIS WEBSITE.

L'accès à ce site Web et l'utilisation de son contenu sont assujettis aux conditions présentées dans le site

<https://publications-cnrc.canada.ca/fra/droits>

LISEZ CES CONDITIONS ATTENTIVEMENT AVANT D'UTILISER CE SITE WEB.

**Questions?** Contact the NRC Publications Archive team at

PublicationsArchive-ArchivesPublications@nrc-cnrc.gc.ca. If you wish to email the authors directly, please see the first page of the publication for their contact information.

**Vous avez des questions?** Nous pouvons vous aider. Pour communiquer directement avec un auteur, consultez la première page de la revue dans laquelle son article a été publié afin de trouver ses coordonnées. Si vous n'arrivez pas à les repérer, communiquez avec nous à PublicationsArchive-ArchivesPublications@nrc-cnrc.gc.ca.



# OPTICAL COHERENCE TOMOGRAPHY USED FOR JADE INDUSTRY

Shoude Chang<sup>1</sup>, Youxin Mao<sup>1</sup>, Guangming Chang<sup>2</sup>, and Costel Flueraru<sup>1</sup>

<sup>1</sup>Imaging Devices Group, Institute for Microstructural Sciences  
National Research Council Canada, Ottawa, Ontario, Canada K1A 0R6

<sup>2</sup>Shandong Yingcai University, Jinan China

## ABSTRACT

As an expensive natural stone, jade has a worldwide market. In the jade industry, the inspection and analysis basically rely on the human eye and/or experience, which cause unavoidable waste and damage of these expensive materials. Optical Coherence Tomography (OCT) is a fundamentally new type of optical sensing technology, which can perform high resolution, cross-sectional sensing of the internal structure of materials. As jade is almost translucent to infra red light, OCT becomes an ideal tool to change the traditional procedure to volume data based machine vision system. OCT can also be used for anti-counterfeit of the expensive jade ware.

**Key words:** optical coherence tomography, jade estimation, texture analysis, artwork diagnostics, pattern recognition.

## 1. INTRODUCTION

Optical coherence tomography (OCT) is a powerful imaging technology for producing high resolution cross-sectional images of the internal microstructure of materials and biological samples. It has been widely used in medical exam and biological testing for more than ten years [1-3]. It relies on the interferometric measurement of coherent back scattering variation to form images of the surface structure of test samples like biological tissues or other turbid materials. It takes advantage of the short temporal coherence of a broadband light source to achieve precise optical sectioning in the depth dimension.

Comparing to other imaging technologies, OCT has unique features as followings. 1) High resolution. Resolution for different systems: OCT, 5-10 microns; ultrasound, 150 microns; High resolution CT, 300 microns; MRI, 1,000 microns. This feature enables greater visualization of defects. 2) Noninvasive, non-contact detection. This feature increase safety and ease of use and extends the possibility for *in vivo* applications, which is important for biomedical applications. 3) Fiber-optics delivery. As fiber diameter is normally 125 microns, it allows OCT to be used in catheters and endoscopes. It also creates another new feature of OCT: imaging while treating. 4) High speed. The new generation of OCT technology has no mechanical scanning procedures, which enables high-resolution 3D imaging, particularly for the full-field OCT. 5) Potential for additional information of the testing sample. The new optical property of tissues could be explored by functional OCT. For examples, polarization contrast, Doppler effects, as well as spectroscopic information can be obtained concurrently from the testing tissues.

6) Use of non-harmful radiation. OCT systems work with visual and infrared band, unlike traditional CT working with X-ray and ultrasound relying on mechanical vibration.

In the past decade, OCT systems have been developed mainly for medical and biomedical applications, especially for the diagnostics of ophthalmology, dermatology, dentistry and cardiology. To explore the capabilities of OCT system for probing the internal features of an object, references [4,5] reported the applications for multiple-layer information retrieval and internal biometrics [6,7]. In addition, because OCT has the voxel resolution of micrometer size, it has potential applications in material investigation [8] and artwork diagnostics. Reference [9] describes OCT diagnostics used for museum objects, involving stratigraphic applications; varnish layer analysis; structural analysis and

profilometric applications. This paper describes the OCT technology applied to jade industrial. Based on statistical analysis of the OCT data, the existence and quality of jade can be detected and estimated.

## 2. SWEPT-SOURCE OPTICAL COHERENCE TOMOGRAPHY

OCT relies on the interferometric measurement of coherent back scattering variation to sense the surface structure of test samples like biological tissues or other turbid materials. It takes advantage of the short temporal coherence of a broadband light source to achieve precise optical sectioning in the depth dimension.

Time domain OCT system is based on a Michelson interferometer. In time-domain OCT (TD OCT) systems, broadband source is used in interferometer. The coherent gate is then created to separate the tomography at a certain layer. A mechanic scanning device is used to select difference layer at different depth by moving the reference mirror. The scanning procedure basically determinates the processing speed of the whole system.

As the scanning procedure in TD OCT is actually a procedure of convolution, it can be expressed by

$$Id \propto Es \otimes Er, \quad (1)$$

where  $Es$  and  $Er$  are the electronic fields from source and reference arms, respectively. Its Fourier transform becomes

$$Id(\omega) \propto s_s(\omega) \bullet s_r(\omega). \quad (2)$$

Where,  $s_s(\omega) = \frac{1}{2} s(\omega)$ ,  $s_r(\omega) = \frac{1}{2} s(\omega)$ ,  $s_r(\omega)$ ,  $s_s(\omega)$  are Fourier transform of  $Es$  and  $Er$ , respectively.  $s(\omega)$  is the light source spectrum. Considering the interferometer structure, the signal detected by sensor is given by

$$Id(\omega) = |s_r(\omega) + s_s(\omega) \bullet s_r(\omega)|^2 = S(\omega) [1 + s_s(\omega)]^2, \quad (3)$$

where,  $S(\omega) = s^2(\omega)$ .

Equation (3) is the foundation of Fourier Domain OCT (FDOCT) or Spectral Domain OCT (SDOCT) [10,11]. SDOCT extracts the spectral signal by means of a grating spectrometer and a linear detector-array. The reconstruction of the internal tomography is performed by an inverse Fourier transform of  $Id(\omega)$ . Instead of using a broadband light source, the Swept Source OCT (SSOCT) uses a swept-wavelength laser as the light source. SDOCT gets all the broadband  $Ids(\omega)$  in one shot but collects the signal in series from the linear detector array. However, SSOCT collects the spectral signal in series by changing the wavelength of the light source. Both need an additional inverse Fourier transform, implemented by either hardware or software.

FDOCT and SDOCT have several advantaged over TDOCT. Because of no mechanic scanning, the FDOCT system is significantly faster, 50 to 100 times, than TDOCT. In addition, both FDOCT and SSOCT have better sensitivity and signal noise ratio [12].

In Swept-Source Optical Coherence Tomography (SSOCT), the broadband light source plays an important role. The linewidth and output power determinate the imaging range of an SSOCT system. The bandwidth of the light source places the main barrier for the imaging resolution. At current stage, most commercial swept-sources have a bandwidth about 100 nm corresponding to an axial resolution around 14  $\mu\text{m}$  in air.

In SSOCT, the swept-source stimulates the system by a series of wavelengths in time sequence; a photo detector then collects all the responses as Fourier series components of testing sample. Because the detector is only sensitive to optical energy, it loses the phase information in the reflected/back scattered signal. At any moment, the signal detected by sensor can be written like this:

$$I(k) = |E(k)H(k)|^2, \quad k = 1,2,3,4 \dots N. \quad (4)$$

Where,  $E(k)$  is the  $k^{\text{th}}$  wavelength sent from source,  $H(k)$  represents the overall reflection from testing sample, and  $I(k)$  is the signal generated by the sensor. Assuming  $S(k) = |E(k)|^2$ , power spectrum of the light source, the output of an interferometer based OCT system can be expressed by:

$$\square \quad I(k) = S(k) [ H(k) + 1 ]^2 . \quad (5)$$

Extending (5),  $I(k) = S(k) H^2(k) + 2S(k) H(k) + S(k)$ . Taken  $S(k)$  as a constant and  $H^2(k)$  as low frequency component that can be ignored, the processed  $I(k)$  becomes

$$Ip(k) = C H(k), \quad (6)$$

C is a constant.

The reconstruction of the sample in spatial domain (depth  $z$ ) is performed by an inverse Fourier transform:

$$h(z) = \text{IFT} [ Ip(k) ] . \quad (7)$$

At any moment, as Equation (6)(7) are the results from one wavelength,  $h(z)$  is a flat curve, meaning one Fourier component can not build a structure. However, if all the  $Ip(k)$ s with different wavelengths form a sequence,

$$Is(k) = \sum_n Ip(k) \delta(k-n), \quad n=1, 2, \dots, N, \quad (8)$$

the internal structure of the sample can then be extracted by

$$h(z) = \text{IFT} [ Is(k) ] = \text{IFT} [ \sum_n C H(k) \delta(k-n) ] . \quad (9)$$

Where,  $\delta(k-n)$  is used to separate each Fourier series component at a discrete  $k$  number.

### 3. JADE AND JADE INDUSTRY

Jade can be classified into two groups: nephrite jade or jadeite jade. Nephrite jade, (a silicate of calcium and magnesium), is the historical Chinese Jade, or Stone of Heaven, a stone revered by the Chinese for more than 5000 years. Nephrite is prized for its special qualities: its extreme toughness, (the toughest of any natural stone), its alluring translucency and a smooth polished feeling. Colors of Nephrite Jade range from pure white to all shades of green.

Jadeite Jade, (silicate of sodium and aluminum), a relatively new jade introduced to China from Burma in 1784. Gem quality Jadeite is extremely rare and thus extremely expensive. Often mislabeled as "Chinese jade," (it was never found in China), jadeite is slightly harder than nephrite jade. Jadeite is often color enhanced. Colors of jadeite range from white to black with intense greens and lavender being the most sought after.

Jade is a kind of expensive natural stone. Its price directly depends on the quality of the material, as well as the beauty of the finally carved artwork. In Chinese market of 2007, a high quality "Hetian" jade costs about US\$125,000/kg. The most expensive "Hetian Yangzhi" jade has the price as high as USD\$1,250 /gram.

Jade has a huge market in worldwide, particularly in Asia countries, including Burma, Thailand, Korea, Japan and China. In Guangdong province of China, the annual sale exceeds USD\$100M. In Canada, a company named Jade West, is one of the world's largest producers and exporters of nephrite jade, which annually mines 100 tons of jade for export.

There are 4 distinct steps in the procedure of jade: Exploration, Breaking Out, Cutting, and finally, Artistically Carving.

- Exploration. This process involves drilling into the mountain side with water cooled diamond tipped core drills. The cores are then extracted and examined to determine if the jade will meet the gem grade requirements suitable for the finished products and gem stones.

- **Breaking Out.** After the Jade Cores have been examined and quality has been determined, the miners will analyze the face looking for cleavage points. These natural joints can be exploited to remove the jade. More core holes will be drilled, and heavy hydraulic spreaders will be inserted into these cracks to push the jade apart.
- **Cutting.** After the jade boulders have been broken out, they are then taken to huge diamond saws to be reduced to manageable sizes. The sawyer will also cut windows into the boulder to better expose the beautiful jade within.
- **Artistically Carving.** The jade sculptors will finally make the raw jades, small or big, into art crafts. Because normally marks and textures exist inside the raw jade, they create a lot of challenges and opportunities to the artist in designing and carving. A beautifully carved jade should maximally use the jade material and creatively borrow the internal aliens.

#### **4. OCT TECHNOLOGY APPLIED TO JADE PROCEDURE**

Optical Coherence Tomography (OCT) is a high resolution, non-destructive, imaging technique developed in the last decade. It can be used to explore the internal structure of an object in micro meter level. Recently, we have used OCT to extract the tomographic images of different types of jades. The experimental results show that the internal structures, including the marks, textures at different depths, can be observed clearly within 4 mm depth (see Pictures part I). And also, we noticed that there is about 20dB difference of the OCT signal intensity between jade and its wrapping materials.

These results show that the OCT technology can be applied to the jade industry. Almost all the 4 steps of the jade procedure can be greatly facilitated, and in addition, it can efficiently avoid the waste in raw material preparing as well as failures in artistically carving, with the help of an OCT system.

In the Exploration step, the cores can be examined by OCT system. Instead of cutting off a large area at the core for visual observation, a small hole is drilled into the core and then a tiny fiber probe of OCT is inserted to analyze if the jade is there and what is the type and quality of the jade. In Breaking Out step, OCT technology can also be used to find the natural joints or flaws inside the core for cleavage. It will greatly reduce the waste of material and increase the accuracy of the quality analysis.

In Cutting step, to explore the beauty inside, the normal way is cutting a window into the boulder. However, this blindly bulk trials definitely waste and damage the jade, particularly when the jade is a high quality one. However, by using an OCT system, it will reduce the waste and damage to the minimal level.

In the last step, Artistically Carving, the most annoying issue is that the artist has to guess what is hidden underneath the surface of the jade, especially the existence and features of the marks and textures. If the guess is wrong, an almost perfect art work may be destroyed and devalued by the unknown internal structure at the last minute. However, with the help of the OCT system, the sculptor can see through the material in depth and therefore, successfully guide the jade carving.

Another potential application is the discrimination of the fake antique jadewares, which is critical in the antique market. The real ancient jade always carries some ooze and deposit on / under the surface, after hundreds or thousands years burial. The penetration features, for examples, depth distribution and pattern, are different between the real one and fake one. These features can be detected by an OCT system with specially developed algorithms.

In addition, even for the expensive modern jade, there are so many counterfeiters on the market. OCT technology could also be used to recognize the artificial ones by analyzing the optical and structural features. For example, the miniature air bubbles exist inside many manmade jades that are normally invisible by human eyes, however, being able to detect these miniatures at a micro meter level, is the strength of OCT systems.

## 5. JADE DETECTION AND ANALYSIS

The OCT setup used in experiments is illustrated in Figure 1. The swept source is a commercially available swept laser with a scanning frequency of 20 kHz, a spectral range of 110 nm centered at 1320 nm and an optical power of 10 mW (SANTEC, Japan). The light is directed through a 2 x 2 fibre coupler on the reference mirror and the sample arm. The optical tip is mounted on a galvo-scanner, which focuses the light on the sample through a fibre ball lens. The back scattered / reflected signals from both mirror and sample are input into a second 2 x 2 fibre coupler configured in a

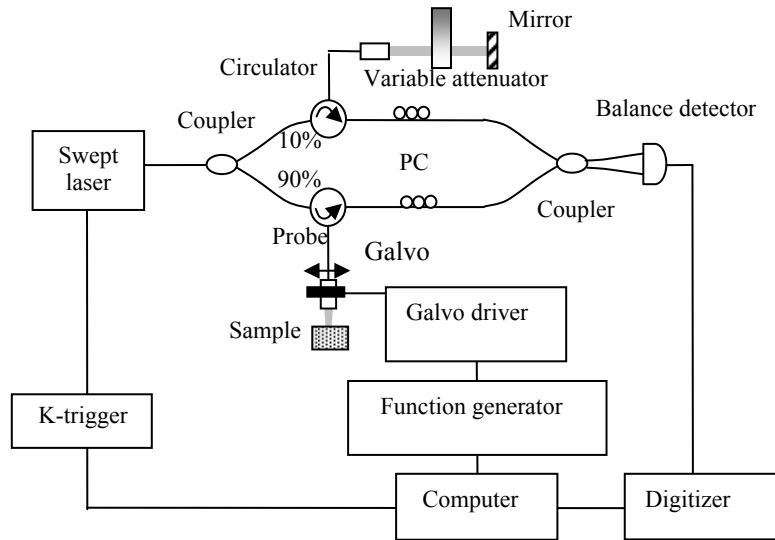


Figure 1. Swept-Source OCT used in experiments

Mach-Zehnder geometry. Its two outputs become the input in a balanced detector (New Focus). The output of balanced detection is recorded with a digitizer (Alazartech) at a 100 MHz sampling rate. The signal is re-sampled to equal frequency intervals and subjected to an inverse Fourier transform. The resolution of the setup is 7  $\mu\text{m}$  for axial direction.

In order to find the optical property of a jade, we firstly measured the intensities of OCT signal reflected or back scattered from the jade body and non-jade material deposited on surface. The photo inside Fig. 2(a) shows a jade (dark green-like) with some deposit (white-like) material wrapped on it. Two OCT A-scans (depth scan), A-scan 1 and A-scan 2, were performed upon the non-jade area and jade body area. Figure 2(b) and (c) show the plots of A-scan 1 and A-scan 2 signals, respectively. In these plots, the first peak represents the DC component, the second peak results from interlayer interference. The third peak is caused by the surface of the testing object. It is easy to see that there is about 20dB difference in the OCT signal intensity between jade and non-jade materials. Hence, the intensity of the OCT signal provides an effective indication for detecting the jade presence. In this case, the threshold can be set as -40 dB.

To explore the internal structures, different types of jades, numbered 1-6 shown in Fig.3 were then tested. Differing to the en-face image, the A-scan OCT image contains some open-air area, which is non-object and needs to be removed before doing texture analysis. We have designed a two-step algorithm to segment the object area. In the first step, a binary mask was created by finding the maximum points in each vertical line (A-scan line). Because the maximum pixel may not be located at the object border, the second step is needed to remove these vertical thorns. The segmented OCT image is called SgOCT image, in which the pixels in open-air area are not counted in jade analysis, as shown in Figure 4.

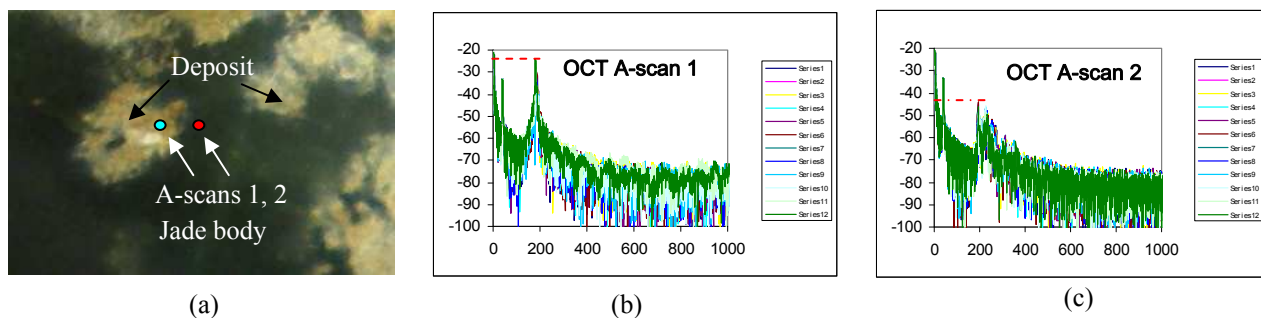


Figure 2. Two A-scans on jade body and non-jade material

To explore the internal structures, different types of jades, numbered 1-6 shown in Fig.3 were then tested. Differing to the en-face image, the A-scan OCT image contains some open-air area, which is non-object and needs to be removed before doing texture analysis. We have designed a two-step algorithm to segment the object area. In the first step, a binary mask was created by finding the maximum points in each vertical line (A-scan line). Because the maximum pixel may not be located at the object border, the second step is needed to remove these vertical thorns. The segmented OCT image is called SgOCT image, in which the pixels in open-air area are not counted in jade analysis, as shown in Figure 4.

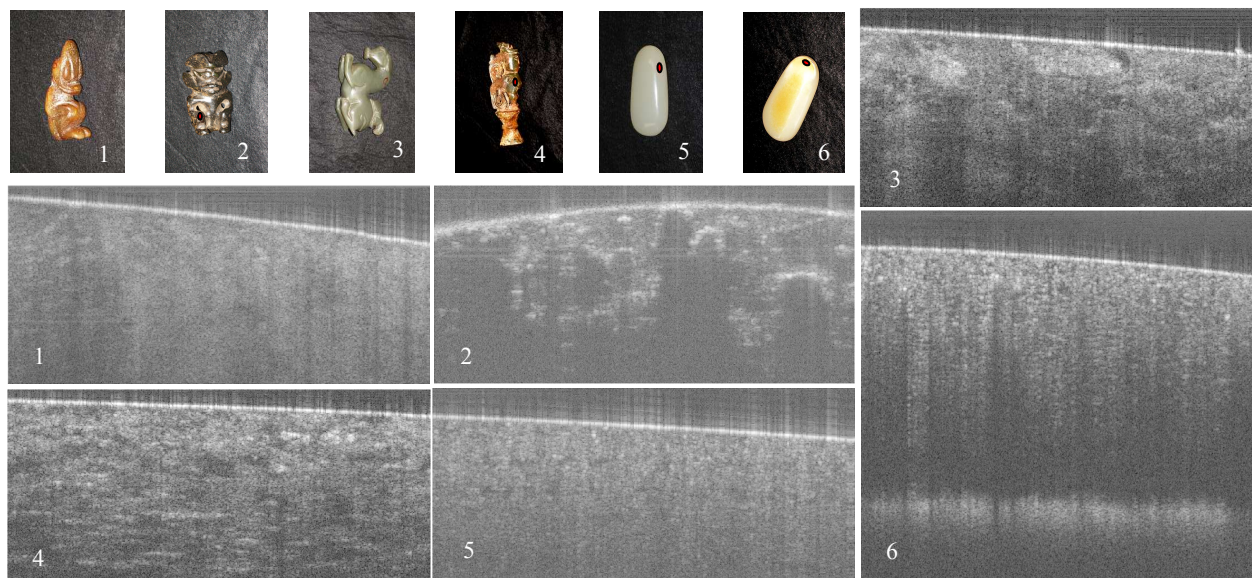


Figure 3. Six jades and their OCT A-scan images, numbered as Jade #1, Jade #2, Jade #3, Jade #4, Jade #5 and Jade #6

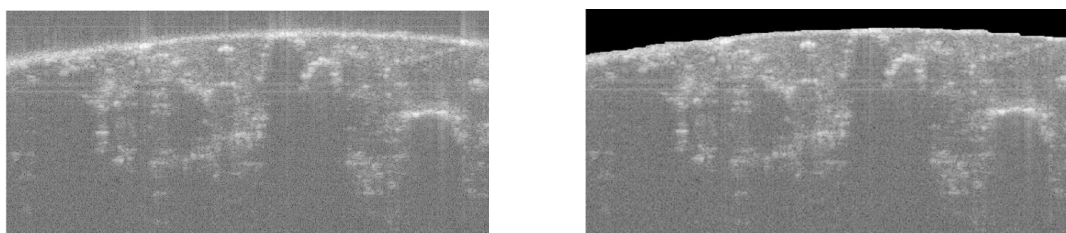


Figure 4. Jade OCT image before (left) and after (right) segmentation

Reference [13, 14] reported different methods to analyse the texture features, especially for the biology samples. The textures of jades are significantly different from those in biomedical OCT images. They almost have no continuous edges, solid borders, or closed sub areas inside. They look more like galaxy patterns. Hence, statistics may be the only tool for texture feature description. In this work, we proposed to extract six parameters from an A-scan OCT image. They are 1) Entropy of the SgOCT image; 2) Half-peak width of the histogram of the SgOCT; 3) Standard deviation of histogram of SgOCT; 4) Average gray value of SgOCT; 5) Standard deviation of SgOCT; 6) Variance of SgOCT.

Entropy of the SgOCT image is calculated based on the histogram of SgOCT image:

$$E_{tr} = \sum_i -\log_2[H_{his}(i)] \cdot [H_{his}(i)], \quad (10)$$

where,  $H_{his}()$  is the histogram of SgOCT,  $i$  represents the individual grey level in SgOCT.

Table 1 provides the values of these parameters of six jades shown in Figure 3. For each set of parameters, all the values are normalized from 0 to 1, which was done by subtracting the minimum and then dividing by the maximum.

Six-parameter can form a texture vector:

$$\mathbf{V}_i = a_1 f_{1i} \mathbf{v}_1 + a_2 f_{2i} \mathbf{v}_2 + a_3 f_{3i} \mathbf{v}_3 + a_4 f_{4i} \mathbf{v}_4 + a_5 f_{5i} \mathbf{v}_5 + a_6 f_{6i} \mathbf{v}_6, \quad i = 1, 2, \dots, 6, \quad (11)$$

where,  $f_1 - f_6$  are the normalized values of parameters in Table 1.  $\mathbf{v}_1 - \mathbf{v}_6$  are the unit vectors representing each parameter, respectively. Table 2 gives the variances of each parameter for different jades.  $a_1 - a_6$  are weighting factors, whose values are given by the order of the values of variances. For example, the parameter with the maximal variance has a weighting factor 6, and the one with minimal variance has a factor 1, simply because we have six vector components. All these weighting factors are listed in the send row of Table 2.

Table 1. Normalized values of 6 parameters

		Jade 1	Jade 2	Jade 3	Jade 4	Jade 5	Jade 6
$f_1$	Entropy	0.2941	0.2618	1.0000	0.2471	0.3088	0
$f_2$	Half peak width	0.6543	0	1.0000	0.6543	0.6162	0.1924
$f_3$	Std. dev. entropy	0.5972	0.8665	0	0.6573	0.6198	1.0000
$f_4$	Av. gray image	0.8160	0.6748	0.6288	1.0000	0.6656	0
$f_5$	Std. Dev. image	0	0.1882	0.5926	0.2750	0.2103	1.0000
$f_6$	Var. of image	0.6024	0.6491	0	0.6298	0.5987	1.0000

Table 2. Variances and weighting factors for each vector components

	$f_1$	$f_2$	$f_3$	$f_4$	$f_5$	$f_6$
Variance	0.1136	0.1307	0.1183	0.1143	0.1301	0.1042
$a_i$	2	6	4	3	5	1

The intensity of the texture vector of jade #i is given by

$$|\mathbf{V}_i|^2 = \sum_j (a_j f_{ji})^2, \quad j=1, 2, \dots, 6, \quad (9)$$

which can be used to numerically distinguish the type of jade. The intensities of texture vector of six jades used in experiments are given in Table 3 and Fig. 5. From these results, six jades can be classified at different  $|\mathbf{V}_i|^2$  values. Among them, jade #1 and #5 have closed values. Looking at their OCT images in Fig. 3, apparently, the textures of these two jades look kind of similar.

Table 3. Intensities of texture vector for six jades

	Jade 1	Jade 2	Jade 3	Jade 4	Jade 5	Jade 6
$ \mathbf{V} ^2$	27.8189	17.6935	52.3397	33.8558	25.6501	43.3324

## 5. SUMMERY AND DISCUSSION

Optical coherence tomography paves a new avenue for exploring and analysing the internal structure of an object. The micron level resolution makes it unique to other tomographic imaging technology. OCT technology has potential applications to many fields, including medical, security, environment, and industrial. In this paper, we have briefly described the principle of Swept-Source OCT systems and shown the possibility of their application in jade exploration and analysis.

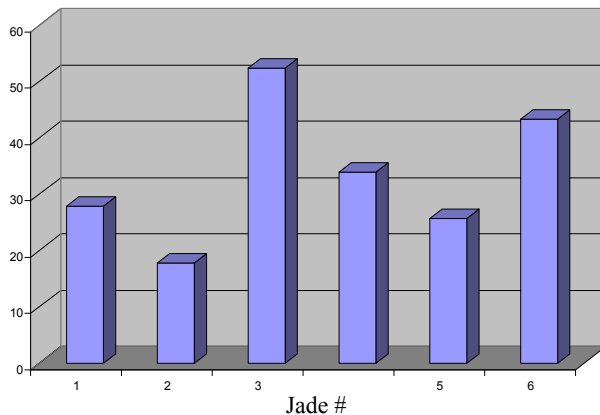


Figure 5. Six intensities of texture vector calculated from 6 jades

Because the jade is almost translucent to the IR light and has internal texture associated with different type, this property can be used to detect the presence of jade. Experiments show that there is a big difference, around 20 dB, of the reflected/back scattered OCT signals between the jade body and the non-jade wrapping material. And also, almost no structure is detected in the non-jade material in the depth due to the weak signal. Based on the jade samples we currently have, we proposed a texture analysis method upon their OCT signal. Six parameters were used to numerically describe the texture pattern of the jades. To the best of our knowledge, it is the first time, the internal crossing-sectional structure and texture of jade materials is extracted and analyzed. Experimental results show that the OCT technology could be a useful tool for the jade

exploration and analysis by machine vision. For example, by drilling a tiny hole in the boulder of jade, and placing a fibre probe into it, the OCT system can provide a solution if there is jade inside and what kind of the type it could be. It will greatly facilitate the traditional jade procedure. In addition, with the help of an OCT system, it could avoid the waste in raw material preparing as well as reduce the risk in artistically carving. Another important application is the anti-counterfeiting of the expensive jadeware. Although authors in Ref. [15] described the OCT signal difference between the real and fake jade in the whitening areas, actually, it is not enough for advanced counterfeit antique jade. The real ancient jade always carries some ooze and deposit beneath the surface, after burial for hundreds or thousands of years. The features of these substances extracted by OCT may provide a powerful tool to distinguish the real antique jade.

## REFERENCE

- [1] D. Huang, E. A. Swanson, C. P. Lin, J. S. Schman, W. G. Stinson, W. Chang, M. R. Hee, T. Flotte, K. Gregory, C. A. Pullaifito, J. G. Fujimoto, "Optical Coherence Tomography," *SCIENCE*, 254, 1178-1181 (1991).
- [2] W. Drexler, J. G. Fujimoto: *Optical Coherence Tomography, technology and Applications*. Springer-Verlag Berlin Heidelberg, 2008.
- [3] G. Smolka, *Optical Coherence Tomography: Technology, Markets, and Applications 2008-2012*. BioOptics World. Penn Well Corporation, 2008.
- [4] Shoude Chang, Xinping Liu, Carl Cai, and Chander P Grover, "Full-field optical coherence tomography and its application to multiple-layer 2D Information retrieving", *Optics Communications* 2005, 246, 579-585 (2005).
- [5] S. Chang, X. Cai, and C. Fluerau, "Image enhancement for multilayer information retrieval using full-field optical coherence tomography," *Applied Optics*, 45(23), 5967-5975 (2006).
- [6] Y. Cheng, and K. V. Larin, "Artificial fingerprint recognition by using optical coherence tomography with autocorrelation analysis", *Applied Optics*, 45, 9238-9245 (2006).
- [7] S. Chang, Y. Cheng, Kirill V. Larin, Y. Mao S. Sherif and C. Fluerau "Optical coherence tomography used for security and fingerprint sensing applications," *IET Image Processing*. V2, N1, 48-58 (2008).
- [8] K. Wiesauera, M. Pircherb, E. Götzingerb, S. Bauerc, R. Engelked, G. Ahrensd, G. Grütznard, C. K. Hitzenbergerb, D. Stiftera, "En-face scanning optical coherence tomography with ultra-high resolution for material investigation," *Optics Express*, 13,3, 1017-1024 (2005).
- [9] P. Targowski, M. G' ora, and M. Wojtkowski, "Optical Coherence Tomography for Artwork Diagnostics," *Laser Chemistry*, DOI:10.1155/2006/ 35373. Article ID 35373, 11 pages (2006).
- [10] S. R. Chinn, E. A. Swanson, J. G. Fujimoto, "Optical coherence tomography using a frequency-tunable optical source," *Opt. Lett.*, 22, 340-342 (1997).
- [11] S.H. Yun, S. H. Yun, G. J. Tearney, J. F. de Boer, N. Iftimia and B. E. Bouma, "High-speed optical frequency-domain imaging," *Opt. Exp.* 11, 2953-2963 (2003).
- [12] J. F. de Boer, et al. "Improved signal-to-noise ratio in spectral-domain comared with time-domain optical coherence tomography," *Opt. Lett.* 28, 2067-2069, ISSN: 0146-9592. (2003).

- [13] M. Oberholzer, M. Ostreicher, H. Christen, and M. Bruhlman, "Methods in quantitative image analysis," *Histochem Cell Biol.* 105, 333-355 (1996).
- [14] K. W. Gossage, T. S. Tkaczyk, J. J. Rodriguez, and J. K. Barton, "Texture analysis of optical coherence tomography images: feasibility for tissue classification," *Journal of Biomedical Optics.* 8(3), 570-575 (2003).
- [15] M. L. Yang, C. W. Lu, I. J. Hsu, and C. C. Yang, "The use of optical coherence tomography for monitoring the subsurface morphologies of archaic jades," *Archaeometry.* 46(2), 171-182 (2004).